Light, transpiration and water use efficiency: contrasts among seedlings of three *Eucalyptus urophylla* × *Eucalyptus grandis* clones s

Abstract

Accurately measuring water absorption and consumption can help improve understanding of forest dynamics and water resource management, especially in areas with water restrictions. In this study, the objective was to evaluate hourly, daily and accumulated transpiration rates of young *Eucalyptus urophylla* × *Eucalyptus grandis* plants. A randomized block experiment was conducted with seedlings of clones I144, CO1407, and A211 transplanted into pots. At 120 days after transplanting, leaf area and root, shoot, and total dry mass were measured. Furthermore, water use efficiency, the relationship between transpiration and leaf area, and the relationship between daily transpiration and energy availability, provided by radiation balance and leaf area ratio, were determined. Leaf transpiration increased concomitantly with plant growth of all clones, reaching a maximum with the highest leaf area. The volume of water consumed at the end of 1689 accumulated degree-days was around 20% higher in clone I144, compared to clones CO1407 and A211. The clones showed differences in hourly transpiration throughout the growth stages. CO_2 assimilation varied between clones, with net photosynthesis being higher in clone A211, while clones I144 and CO1407 showed higher quantum yield. The increase in leaf area helped to increase the transpiration rate and improve the efficiency of using the energy balance for water loss from the plants. Dry mass production and partitioning were higher in clones I144 and A211. Conversely, regarding water use efficiency, clones A211 and CO1407 had higher dry mass yield per gram of water transpired. Thus, we conclude that, among the most productive clones, clone I144 was preferably recommended for areas free from water restrictions, while clone A211, for areas with low water availability.

Key-words: water use efficiency, plant growth, leaf area, net photosynthesis, quantum yield, plant-water relationship

Introduction

Eucalyptus spp. is a very important forest species for the economy of many countries, and its plantations extend over 25 million hectares in several tropical and subtropical regions of the world (Silva et al., 2020; Martins et al., 2022). For instance, in Brazil, it is the most planted forest species (Bassaco et al., 2018), and its continuous expansion is supported by breeding programs and intensive silvicultural practices, which have contributed to increasing its productivity approximately four times in 50 years, currently reaching 38 $m^3 . ha^{-1} . year^{-1}$ (Binkley et al., 2017; Fernández et al., 2018, Ibá, 2022). For greater productivity, an increasing requirement for natural resources is necessary, particularly the water supply (Hakamada et al., 2020). Nevertheless, *Eucalyptus* plantations have expanded to regions that even include areas with scarce and unstable rainfall (Binkley et al., 2017; Scolforo et al., 2019). Furthermore, in recent years, climate change has also caused unusual droughts in traditional *eucalyptus* plantation areas (Otto et al., 2015). Therefore, selecting species and genotypes that combine high biomass production and lower water use has been a challenge for *Eucalyptus* breeding programs aiming to adapt them to areas with limited water supply (Bouvet et al., 2020).

Water use by *Eucalyptus* plantations has been a controversial topic throughout the world over time, due to its effect on local water resources (Almeida et al., 2010). *Eucalyptus* stands are usually planted in a short-term rotation system, in which canopy closure occurs 2-3 years after planting, and around 4 years are required for biomass generation, and 6-7 years for cellulose production. Successive planting and harvesting over large areas in a short term are often associated with higher transpiration rates than slower growing species (Hubbard et al., 2010). Given that *Eucalyptus* plantations have expanded very quickly in Brazil, information is increasingly needed on how management intensity and forest productivity influence water use by these plantations.

Leaf transpiration naturally results mainly from stomatal opening to acquire atmospheric CO_2 to be used in the photosynthetic process. Therefore, this water loss in the form of vapor is an inevitable consequence of photosynthetic carbon gain, making it the main water discharge route from forests (Muñoz-Villers et al., 2018; Han et al., 2019; He et al., 2020). Plants that have high CO_2 absorption rates often show high transpiration rates, which leads to high water requirements (Klar, 1984; Stape et al., 2004; Nguyen et al., 2023). Furthermore, the transpiration rate is strongly influenced by variation in the

microclimate, such as energy balance, soil moisture and by physiological and structural properties of the species, such as root system depth, hydraulic architecture, leaf area and tree height (Rossatto et al. al., 2012; Zhang et al., 2018; Nan et al., 2019).

Understanding how water use by fast-growing species varies over time, and how consumption can be analyzed at different scales, from individual trees to stands or landscapes, can be crucial for deciding on land management and, potentially, for selecting a clonal stock that brings together the best characteristics. An accurate measurement of transpiration can help forest managers plan strategies to make *Eucalyptus* plantations more sustainable. Furthermore, this knowledge will be useful for predicting forest dynamics and managing water resources, especially in areas with low water availability (Han et al., 2019). In this study, we aimed to measure the transpiration rate of three commercial *Eucalyptus* clones from crossing *Eucalyptus urophylla* × *Eucalyptus grandis*. Our main hypotheses were: (i) there are differences in relation to water use between these clones and (ii) external factors and plant characteristics drive the transpiration rate of clones.

Material and methods

Site description and experimental design

A pot experiment was conducted in a non-protected and open-air area of the Department of Forestry and Wood Sciences, at the Federal University of Espírito Santo, in Jerônimo Monteiro city, Espírito Santo state, Brazil (20º47'S, 41º23'W, 120 m asl), from May 16th to September 12th, 2021. The local climate is tropical *Cwa* type (dry winter and rainy summer), according to the Köppen-Geiger classification, with average annual precipitation of 1104 mm and average annual temperature of 24.1 °C (Alvares et al., 2013). During the experimental period, the average minimum and maximum temperatures were 16.6 °C and 31.3 °C, respectively, the average daily global radiation was 15.90 MJ m^{-2} day^{-1} and the average vapor pressure deficit was 0.92 kPa (Figure 1).

Meteorological data were monitored by an automatic station, equipped with a datalogger (CR-1000 Campbell Scientific, Inc., Logan, UT, USA) powered by a 12 volt battery, connected to a solar panel programmed to measure global solar radiation (Pyranometer SP – LITE, Kipp & Zonen B.V.,

Delft, The Netherlands), photosynthetically active radiation (PAR LITE, Kipp and Zonen B.V., Delft, The Netherlands), air temperature and humidity (CS500 Campbell Scientific Inc., Logan, UT, USA), wind speed (03001, RM Young; Campbell Scientific, Inc., Logan, UT, USA), and precipitation (TB4, Campbell Scientific Inc., Logan, UT, USA). Readings were recorded every ten seconds, and average values were stored every five minutes. From the temperature and relative humidity data, the vapor pressure deficit (VPD) was calculated, based on the difference between the water vapor saturation pressure and the partial vapor pressure, following the method proposed by Pereira et al. al. (2002).

Thermal weather measurements were based on air temperature data provided by a meteorological station close to the experiment during the experimental period. Degree-day measurements (°C day) were based on minimum, maximum, and basal temperatures below 10 ºC (Martins et al., 2007). The accumulated degree-days (ADD) corresponded to the sum of degree-days since the day of seedling transplanting (Arnold, 1960).

A randomized block design and three *Eucalyptus* clones were used as fixed effects, with four replications and one plant per pot, totaling 12 experimental units. The following clones of *Eucalyptus urophylla* × *Eucalyptus grandis* were selected, with variable tolerance to water restriction — a tolerant clone (A211), a sensitive one (CO1407), and one more usually planted (I144) in the region where the experiment was conducted. Seedlings 90 day old, with average heights of 38.67 cm ± 2.31 cm (clone A211), 23.67 cm ± 1.18 cm (clone CO1407), and 25.87 cm ± 1.4 cm (clone I144), respectively, were transplanted into 60 L polyethylene pots (height 43.5 cm, upper diameter 46 cm, and lower diameter 38 cm), containing 50 L of a commercial substrate based on ground pine bark, plus 5.0 g dm^{-3} of a formulated 16-8-12 (+2) fertilizer gradually released. Pot surfaces were completely covered using a styrofoam disc in order to prevent water evaporation from the substrate.

Growing conditions and parameter measurements

After seedlings transplanting, the pots were placed on electronic weighing lysimeters (weighing scale model Prix 2098, Toledo do Brasil, São Bernardo do Campo, São Paulo, BR). Reading and storage pot weight data were performed using specific dataloggers for monitoring lysimeters connected to a

microcontroller (ESP8266, Espressif Systems), allowing communication with up to six lysimeters, via the RS-232 protocol. Storage of pot weight data in each lysimeter was updated every five minutes.

Irrigation was carried out following the gravimetric method, with water supply based on automatic monitoring of lysimeter dataloggers, given that the lysimeter reading on pot weight data at each update indicates water consumption in the period. Throughout the experiment, the plants were irrigated individually at the end of every day, to recover the substrate moisture to close to 90% of the maximum water retention capacity (MWRC). To determine MWRC, 1.0 L samples of substrate were previously dried in a forced air circulation oven and then their weights were quantified. Thereafter, samples were saturated, followed by complete gravitational water drainage. The MWRC corresponded to the difference between the dry and saturated weights in each liter of substrate.

Measurements on the amount of water lost through plant transpiration were carried out using a lysimetric system, consisting of electronic scales with an individual capacity of 60 kg ± 10 g. Measurements on the weight variation of each experimental unit, composed of a plastic pot, substrate, water, and one young *Eucalyptus* plant, were carried out throughout the day every five minutes. Daily transpiration was taken as the difference in pot weight measured between 6:00 am and 6:00 pm, given that water loss through plant transpiration was the mainly cause of weight variation during this period. The transpiration rate was expressed both per hour and accumulated throughout the experiment, as a result of the sum of daily transpiration.

Some biometric parameters were measured weekly. Plant height (H) was measured from the collar to the youngest leaf at the top of the shoot, using a graduated ruler. Stem diameter (D) was measured at the base of the stem, equivalent to the top level of the pot, using a digital pachimeter. Leaf number (LN) was determined by counting the number of fully expanded leaves. Leaf length (LL) measurement was based on the distance between the distal base of the petiole and the terminal end of the leaf. Leaf width (LW) measurement was based on the blade distance between the two largest adjacent leaflets. At 85 days after transplanting (DAT), the canopy diameter was measured, based on two perpendicular cross-shaped measurements in the shadow cast by the canopy, in which the canopy projection area was calculated, considering the canopy to have a cylindrical shape.

Measurements of photosynthesis-related traits were performed at 70 DAT, on healthy and completely expanded leaves from the upper middle third of the shoot, in four plants of each clone, using a portable infrared gas analyzer (IRGA, Li-Cor, model LI-6400), with a block temperature of 25°C, relative humidity of 50% to 60%, and external CO_2 concentration of 400 ppm. A photosynthesis response curve was obtained with a light decrease of 2500; 2000; 1500; 1200; 800; 500; 200; 100; 90; 80; 70; 65; 60; 55; 50; 45; 40; 35; 30; 25; 20; 15; 10; 5; and 0 µmol m^{-2} s^{-1} of photons, with minimum and maximum waiting times of 120 s and 200 s, respectively. Thereafter, the following photosynthetic parameters were measured: maximum net CO_2 assimilation rate (A_{max}, µmol m^{-2} s^{-1} of photons); dark respiration (Rd, µmol m^{-2} s^{-1} of CO_2); apparent quantum efficiency (Φ, µmol CO_2 / µmol photons), light compensation point (LCP, µmol m^{-2} s^{-1} of photons), and light saturation point (LSP, µmol m^{-2} s^{-1} of photons).

At the end of the experiment, 120 days after transplanting, measurements of total leaf area (LA, m^2) were performed using a leaf area integrator model LI-3100 (Li-Cor Inc, Lincoln, Nebraska, USA). Before that, throughout the experimental period, leaf area was estimated based on the equation LA = LN [f (LL × LW)], where: LN = total number of leaves (non-dimensional); f = shape factor (non-dimensional); LL = leaf length; and LW = leaf width — these last two measurements (cm) were obtained from an average of 100 leaves, with different sizes, extracted from different parts of the plant. The "f" factor was determined by a simple regression analysis between the area of each leaf and the product of their respective dimensions.

For dry mass determination, each plant was removed from the pot and sectioned into shoot (leaves and stem) and roots. Soil fragments were completely removed from the roots by washing with running water using a fine-mesh sieve to prevent loss of root material. The plant material was dried in a forced air circulation oven at 65 ºC until its mass became constant, thus obtaining the dry mass of shoot (SDM, g $plant^{-1}$) and root (RDM, g $plant^{-1}$). Total dry mass (TDM, g $plant^{-1}$) was obtained by summing SDM + RDM. The plant's water use efficiency (WUE) was determined based on the quotient between TDM (kg) and the volume of water (m^3) consumed by the plant. Additionally, the relationship between transpiration and leaf area with global solar radiation, temperature and VPD were evaluated every hour, but only on four days with no precipitation and low cloudiness, at 20, 40, 60 and 120 DAT.

Statistical analysis

Measurements on plant height, stem diameter, leaf area, and leaf area/stem diameter ratio were used to establish a mathematical model to estimate seedling development during the experimental period, with degree-day accumulation as an independent variable. Therefore, a three-parameter sigmoidal model was used, given that it is widely used in plant growth models (Cunha and Volpe, 2011; Lin et al., 2014).

Data were subjected to tests to verify the assumption of normality (Shapiro Wilk) and homoscedasticity (Bartlett). They were then subjected to analysis of variance and, when there were significant differences using the F test, means were compared using the Tukey test ($p < 0.05$). Data processing was performed using the R Core Team (2022) version 4.2.2 software.

Results

Leaf transpiration gradually increased as vegetative growth of *Eucalyptus* clones occurred, reaching values close to 10 L per day. Transpiration also increased on days when there was a greater atmospheric evaporative demand. After an accumulation of 1689 degree days, clone I144 had the highest volume of water transpired, reaching 425.82 L plant^{-1}, which was 25.3% and 29.4% higher than those of clones CO1407 (339, 81 L plant^{-1}) and A221 (329.11 L plant^{-1}), respectively (Figure 2).

The concomitant measurements with hourly periodicity of global solar radiation (SR), temperature and VPD, as well as the transpiration for the three clones, under similar atmospheric evaporative demand (at 20, 40, 60 and 120 DAT), together with the leaf area of each clone, allow us to observe a close relationship of environmental variables with transpiration (Figure 3). At 20 DAT, in the three clones, transpiration remained stable below 0.1 L plant^{-1} h^{-1} throughout the day. At 40 DAT, an increase in transpiration up to 0.2 L plant^{-1} h^{-1}, followed by a decrease, was observed from 8 am to 6 pm. At 80 DAT, a marked increase in transpiration followed by a decrease was observed throughout the day, showing a performance similar to that of global solar radiation. This increase in transpiration was more prominent in clone I144 than in clones CO1407 and A211, which were similar. In clones CO1407 and A211, a decrease in transpiration was observed between 11-12 am, suggesting a more accurate

stomatal control over transpiration. Transpiration reached the highest levels at 120 DAT, with peaks around midday in clones I144 and CO1407, and between 8-10 am in clone A211. At 120 DAT, a significant difference between clones was observed for stomatal conductance, which was higher in clone I144 (0.51 mol m^{-2} s^{-1}), followed by clones CO1407 (0.39 mol m^{-2} s^{-1}) and A211 (0.29 mol m^{-2} s^{-1}) (unpublished data).

Biometric parameters such as plant height, stem diameter, and leaf area showed sigmoidal behavior, i.e., an initial smooth increase that evolved into a marked increase with degree-day accumulation. As for the leaf area/stem diameter ratio, this increase became stable after 1122 accumulated degree-days, with no significant differences between the genetic materials (Figure 4). These results suggest a close relationship between vegetative growth and transpiration.

Referring to plant height, a more prominent increase was observed from 1122 ADD, in clones I144 and CO1407, which had a maximum increase of 0.219 and 0.240 cm per degree-day, respectively, followed by clone A211, whose increase was 0.155 cm. A more prominent increase in stem diameter was observed in clone I144 (0.028 cm per degree-day), followed by clones CO1407 and A211 (0.024 cm). As for leaf area, a more prominent increase occurred from 669 ADD, reaching a maximum of 100 cm^2 per degree-day at the end of the evaluation period, however there was no difference between the *Eucalyptus* clones.

In terms of biomass accumulation at the end of the experiment (120 DAT), a significant increase ($p \leq 0.05$) in dry mass of branches, roots and total was observed in all clones, and it was more prominent in clones I144 and A211. On the other hand, water use efficiency, based on the ratio of biomass produced / water consumed by transpiration, was significantly higher in clones A211 and CO1407, compared to I144 (Table 1).

Regarding the characterization of physiological parameters, a higher net photosynthesis rate was observed in clone A211, while a higher quantum yield was observed in clones I144 and CO1407. Regarding dark respiration, light compensation point, and light saturation point, there was no significant difference between the clones (Figure 5, Table 2). However, the compensation points were low and photosynthetic saturation was not reached until levels above natural solar radiation.

Increased water consumption was observed in all clones throughout the experiment, suggesting a close relationship between transpiration and the increase in leaf area. However, the increase in transpiration occurred at variable rates, showing quadratic regression in clone I144 and A211 and linear regression in CO1407 for the plants of this experiment (Figure 6). Considering the initial parts of the three fitted models in the graphs, up to a plant size of 4 m^2 leaf area, the daily transpired water per plant averaged 1.50 L m^{-2} for I144, 1.37 L m^{-2} for A211 and 0.85 L m^{-2} for CO1407.

The influence of leaf area on transpiration can also be noted by observing the fraction of available energy, represented by the radiation balance that was used as latent heat of vaporization. With the increase in leaf area, energy was basically used for transpiration, especially in plants with high leaf area. It was also verified that all clones reached a stable level, characterized by non-linear regression, according to the Gompertz model (Figure 7).

Discussion

Eucalyptus is the most planted tree species worldwide, and soil water availability is one of the main drivers for its productivity. Climate change has often caused restrictions of water resources for agricultural production, which requires new strategies to improve water use efficiency. Therefore, an accurate understanding of the processes that regulate the water use requirement and efficiency is increasingly required, both to plan irrigation and land management, and to choose clones adaptable to areas with restrictions on water supply.

In this study, the increase in transpiration rate was closely related to the increase in leaf area, although with differences between clones in terms of daily transpiration performance. From approximately 60 (DAT), the leaf area began to expand rapidly, thus increasing the number of stomata and the evaporative leaf surface. As a result, there was an exponential increase in leaf transpiration, concomitant with an increase in the photosynthetic capacity of the canopy. However, as transpiration is also regulated by energy availability, it was observed that water consumption stabilized from approximately 90 DAT (> 7 m^2 leaf area in the plants of this study), and did not reach higher levels despite the fact that the leaf area of the plants continued to increase (Figure 2A). This is possibly due to

increase in competition among leaves as leaf area increases, as well as self-shading which reduces temperature, incidental solar radiation and evaporative demand. Atmospheric evaporative demand has been widely regarded as the majority evaporative driving force for water transport along the soil-plant-atmosphere continuum (Zhang et al., 2017; Li et al., 2019). Studies have reported the influence of canopy size on the transpiration rate in trees (Li et al., 2002; Keramatlou et al., 2015; Salazar et al., 2018; Farooq et al., 2019). As gas exchange occurs predominantly in leaves, the leaf area plays an important role in physiological events such as photosynthesis, respiration, and transpiration. The balance between CO_2 absorption and water consumption, influenced by leaf area, can be decisive for the rate of plant growth (Cemek et al., 2011; Valdez et al., 2015, Lv et al., 2024).

In this study, the transpiration rate varied widely among *Eucalyptus* clones, although their leaf areas were similar. We assumed that the higher transpiration rate observed in clone I144 may have been favored by its high stomatal conductance, thus allowing more water absorption and transport from roots to leaves. In this study, the variable that most affected plant transpiration was solar radiation, but when plants are under saturating light and adequate water supply, stomatal conductance is mainly influenced by atmospheric vapor pressure deficit (VPD). During the morning, under low VPD, stomatal opening reaches a maximum, allowing a higher carbon assimilation rate (Qie et al., 2024). Conversely, stomatal performance tends to be optimized when stomatal kinetics respond quickly to environmental fluctuation (Drake et al., 2013; Meinzer et al., 2017). By the way, this stomatal behavior seems to be occurred in clone A211, as its transpiration rate decreased rapidly in response to the increasing VPD at 120 DAT. An induced low leaf hydraulic conductance can help reduce transpiration-related water consumption and prevent hydraulic failures when VPD increases too quickly (Martin-StPaul et al., 2017; Rodriguez-Dominguez; Brodribb, 2020). According to Zhang et al. (2017), the capacity for stomatal control of transpiration tends to vary in *Eucalyptus* clones. Stomata play a central role in the hydrological and carbon cycles, establishing a balance between CO_2 absorption and transpiration in leaves, which is increasingly important for the adaptive processes of species, especially in water-restricted environments (Sussmilch et al. al., 2019; Haworth et al., 2021).

Although a larger leaf area favors CO_2 absorption, this naturally leads to an increase in transpiration and water consumption (Cemek et al., 2011; Yi; Yano, 2023). Therefore, to improve the

plant's photoassimilation system, a greater hydraulic capacity of the xylem is required in order to meet the canopy's water demand. The relationship between xylem hydraulic capacity and transpiration demand can be assessed using the leaf area (LA) to stem diameter (D) ratio (i.e. LA/D). Biggest reason LA/D suggests greater total leaf hydraulic conductivity, since a greater number of leaves connected to the active xylem tends to favor water transport through the xylem to the canopy (Bond et al., 2008; Domec et al., 2012). In our study, *Eucalyptus* clones presented similar leaf area, but the accumulation of biomass in branches (BDM) and roots (RDM) was greater in clones I144 and A211. According to Mattos et al. (2020), variations in growth rates in *Eucalyptus* clones can be attributed to differences in acquisition and efficiency of use of resources for biomass production. Furthermore, as vegetative growth depends on a balance between carbon gains and losses from the processes of photosynthesis and respiration, carbon not consumed by respiration accumulates, increasing plant dry mass (Falquetto-Gomes et al., 2023).

In this study, water use efficiency (WUE) was based on the ratio of biomass accumulation and the amount of water transpired. The highest WUE observed in clone A211, the more drought tolerant clone, followed by CO1407, and I144 to a lesser extent, can be attributed to possible differences between these clones in terms of their ability to transpire less when producing the same amount of biomass. The differences between clones in terms of transpiration rate may have been influenced by variations in stomatal responses to environmental factors, such as solar radiation, vapor pressure deficit and air temperature. According to Zhang et al. (2017), the capacity for stomatal control of transpiration tends to vary in *Eucalyptus* clones. Stomata play a central role in the hydrological and carbon cycles, establishing a balance between CO_2 absorption and transpiration in leaves, which is increasingly important for the adaptive processes of species, especially in water-restricted environments (Sussmilch et al. al., 2019; Haworth et al., 2021). The high efficiency in biomass production, around 4 g/L, shown by the three clones in this study, is within the highest range of those shown by other tree forest species, which usually ranges between 1.4 and 4.2 g/L (Everson et al, 2011; Paris et al., 2018). This makes them suitable for use in commercial plantations, concentrating high biomass production in a small area and in short periods of time, covering the demand for woody biomass while preserving natural areas of native forests.

Furthermore, these variations in WUE may also be attributed to differences between clones in terms of their photosynthetic capacity. The light response curves (Figure 5) suggest an increase in net photosynthesis rate in response to increasing solar radiation. However, the yield of plant biomass depends both on the amount of radiation absorbed by the leaves and on the efficiency in converting and assimilating light energy through photosynthesis (Larcher, 2003; Kabir et al., 2023). The high photosynthetic rates (above 25 µmol CO_2 m^{-2} s^{-1}) of all clones, especially A211, is consistent with the high productivity usually observed in hybrid *Eucalyptus urograndis*, and this can be attributed to its ability to present high photosynthetic rates regardless of the light level. Conversely, the apparent quantum yield was higher in clones I144 and CO1407, compared to A211. These variations suggest that a hybrid may be efficient at capturing sunlight and converting it to chemical energy, but have a low quantum yield, resulting in a low biomass yield per unit of light captured.

In addition, it was observed that the largest fraction of the available energy, represented by the radiation balance, was dissipated in the form of latent heat of evaporation. With the increase in leaf area, energy was basically used for transpiration, especially when plants reached high leaf area. Plant transpiration largely depends on available energy and the interception of net radiation by the plant canopy (Chen et al., 2023). Therefore, it can be assumed that the larger the leaf area, the greater the efficiency of using the energy balance available in the process of water loss through the stomata. Stomata play an important role in controlling transpiration, regulating the balance between CO_2 absorption and water loss (Urban et al., 2017; Ghimire et al., 2018; Muñoz-Villers et al., 2018; Haworth et al., 2021). In short, although clone I144 produced more biomass than the other clones, data on WUE suggest that its planting is preferably recommended for areas where there is no water restriction. Conversely, clone A211, despite showing intermediate biomass production, may perform better under restricted water availability, as it shows higher WUE.

Conclusion

Leaf transpiration of *Eucalyptus* clones is driven by the expansion of the leaf area and largely depends on the available energy and the efficiency of capturing the balance of radiation by the plant canopy. Variable growth rates result from differences between clones in their ability to acquire and use

resources to produce biomass. Each clone's ability to reduce water absorption improves water use efficiency. Clones have varying performances in terms of growth, photosynthetic efficiency and transpiration, which can be useful for selection and appropriate management in commercial plantations. Clone A211 shows potential for cultivation under water restriction.

References

ABRAF. 2013 *Brazilian Association of Forest Plantation Producers*. ABRAF Statistical Year Book – Base Year 2012. Brasília.

Almeida, A. C., Soares, J. V., Landsberg, J. J., Rezende, G. D. 2007 Growth and water balance of *Eucalyptus grandis* hybrid plantations in Brazil during a rotation for pulp production. *For. Ecol. Manag.* **251**, 10-21. https://doi.org/10.1016/j.foreco.2007.06.009.

Alvares, C. A., Stape, J. L., Sentelhas, P. C., De Moraes, G., Leonardo, J., Sparovek, G. 2013 Köppen's climate classification map for Brazil. *Meteorol. Z.*, **22**, 711-728. https://doi.org/10.1127/0941-2948/2013/0507.

Arnold, C. Y. Maximum-Minimum Temperature as a Basis for Computing Heat Units. *Proc. Am. Soc. Hort. Sci.* **76**, 682-692, 1960.

Bassaco, M. V. M., Motta, A. C. V., Pauletti, V., Prior, S. A., Nisgoski, S., Ferreira, C. F. 2018 Nitrogen, phosphorus, and potassium requirements for *Eucalyptus urograndis* plantations in southern Brazil. *New For*. **49**, 681-697. https://doi.org/10.1007/s11056-018-9658-0.

Binkley, D., Campoe, O. C., Alvares, C., Carneiro, R. L., Cegatta, Í., Stape, J. L. 2017 The interactions of climate, spacing and genetics on clonal *Eucalyptus* plantations across Brazil and Uruguay. *For. Ecol. Manag*. **405**, 271-283. https://doi.org/10.1016/j.foreco.2017.09.050.

Bond, B. J., Meinzer, F. C., Brooks, J. R. 2008 How Trees Influence the Hydrological Cycle in Forest Ecosystems. In: Hannah, M. e Sadler J.P. (Eds). *Hydrol. Ecohydrol*. John Wiley & Sons, p. 7-35.

Bouvet, J. M., Ekomono, C. G. M., Brendel, O., Laclau, J. P., Bouillet, J. P., Epron, D. 2020 Selecting for water use efficiency, wood chemical traits and biomass with genomic selection in a *Eucalyptus* breeding program. *For. Ecol. Manag*. **465**, 118092. https://doi.org/10.1016/j.foreco.2020.118092.

Cemek, B., Unlukara, A., Kurunç, A. 2011 Nondestructive leaf-area estimation and validation for green pepper (*Capsicum annuum* L.) grown under different stress conditions. *Photosynthetica*, **49**, 98-106. https://doi.org/10.1007/s11099-011-0010-6.

Chen, Y., Xiao, C., Wu, D., Xia, T., Chen, Q., Chen, F., Mi, G. 2015 Effects of nitrogen application rate on grain yield and grain nitrogen concentration in two maize hybrids with contrasting nitrogen remobilization efficiency. *Eur. J. Agron*. **62**, 79-89. https://doi.org/10.1016/j.eja.2014.09.008.

Chen, D., Hu, X., Duan, X., Wei, X., Zhuo, L., Wang, X., ... & Muhammad, S. 2023 Incorporating dynamic schemes of canopy light extinction coefficient improves transpiration model performance for fruit plantations. *J. Hydrol*. **627**, 130397. https://doi.org/10.1016/j.jhydrol.2023.130397.

Cinnirella, S., Magnani, F., Saracino, A., Borghetti, M. 2002 Response of a mature *Pinus laricio* plantation to a three-year restriction of water supply: structural and functional acclimation to drought. *Tree physiol*. **22**, 21-30. https://doi.org/10.1093/treephys/22.1.21.

Cunha, A.R., Volpe, C. A. 2011 Curvas de crescimento do fruto de cafeeiro cv. Obatã IAC 1669-20 em diferentes alinhamentos de plantio. *Semina: Cien. Agrar*. **32**, 49-61. https://doi.org/10.5433/1679-0359.2011v32n1p49.

Domec, J-C., Lachenbruch, B., Pruyn, M.L., Spicer, R. 2012 Effects of age-related increases in sapwood area, leaf area, and xylem conductivity on height-related hydraulic costs in two contrasting coniferous species. *Ann. For. Sci.* **69**, 17-27. https://doi.org/10.1007/s13595-011-0154-3.

Drake, P. L., Froend, R. H., Franks, P. J. 2013 Smaller, faster stomata: scaling of stomatal size, rate of response, and stomatal conductance. *J. Exp. Bot.* 64, 495-505. https://doi.org/10.1093/jxb/ers347.

Dye, P. J. 2000 Water use efficiency in South African *Eucalyptus* plantations: a review. *South. Afr. For. J*. **189**, 17-26. https://doi.org/10.1080/10295925.2000.9631276.

Farooq, M., Hussain, M., Ul-Allah, S., Siddique, K. H. 2019 Physiological and agronomic approaches for improving water-use efficiency in crop plants. *Agric. Water Manag*, **219**, 95-108. https://doi.org/10.1016/j.agwat.2019.04.010.

Fernández, M., Alaejos, J., Andivia, E., Vázquez-Piqué, J., Ruiz, F., López, F., Tapias, R. 2018 *Eucalyptus* x *urograndis* biomass production for energy purposes exposed to a Mediterranean climate under different irrigation and fertilisation regimes. *Biomass Bioenergy*. **111**, 22-30. https://doi.org/10.1016/j.biombioe.2018.01.020.

Falquetto-Gomes, P., Silva, W. J., Siqueira, J. A., Araújo, W. L., Nunes-Nesi, A. 2023 From epidermal cells to functional pores: Understanding stomatal development. *J. Plant. Physiol*. **292**, 154163. https://doi.org/10.1016/j.jplph.2023.154163.

Ghimire, C. P., Bruijnzeel, L. A., Lubczynski, M. W., Zwartendijk, B. W., Odongo, V. O., Ravelona, M., Van Meerveld, H. J. 2018 Transpiration and stomatal conductance in a young secondary tropical montane forest: contrasts between native trees and invasive understorey shrubs. *Tree physiol*. **38**, 1053-1070. https://doi.org/10.1093/treephys/tpy004.

Gomes, J. M., Paiva, H. N. 2011 *Viveiros florestais*: propagação sexuada. Editora UFV, 116pp.

Hakamada, R. E., Hubbard, R. M., Moreira, G. G., Stape, J. L., Campoe, O., De Barros Ferraz, S. F. 2020 Influence of stand density on growth and water use efficiency in *Eucalyptus* clones. *For. Ecol. Manag*. **466**, 118125. https://doi.org/10.1016/j.foreco.2020.118125.

Han, C., Chen, N., Zhang, C., Liu, Y., Khan, S., Lu, K., Zhao, C. 2019 Sap flow and responses to meteorological about the *Larix principis-rupprechtii* plantation in Gansu Xinlong mountain, northwestern China. *For. Ecol. Manag*. **451**, 117519. https://doi.org/10.1016/j.foreco.2019.117519.

Hatton, T. J., Wu, Hsin-I. 1995 Scaling theory to extrapolate individual tree water use to stand water use. *Hydrol. Process*. **9**, 527-540. https://doi.org/10.1002/hyp.3360090505.

Haworth, M., Marino, G., Loreto, F., Centritto, M. 2021 Integrating stomatal physiology and morphology: evolution of stomatal control and development of future crops. *Oecologia*, **197**, 867-883. https://doi.org/10.1007/s00442-021-04857-3.

He, Q. Y., Yan, M. J., Miyazawa, Y., Chen, Q. W., Cheng, R. R., Otsuki, K., Du, S. 2020 Sap flow changes and climatic responses over multiple-year treatment of rainfall exclusion in a sub-humid black locust plantation. *For. Ecol. Manag*. **457**, 117730. https://doi.org/10.1016/j.foreco.2019.117730.

Hubbard, R. M., Stape, J., Ryan, M. G., Almeida, A. C., Rojas, J. 2010 Effects of irrigation on water use and water use efficiency in two fast growing *Eucalyptus* plantations. *For. Ecol. Manag*. **259**, 1714-1721, 2010. https://doi.org/10.1016/j.foreco.2009.10.028.

IBÁ. 2022 *Relatório anual 2022*. Brasília.

445 Kabir, M. Y., Nambeesan, S. U., Díaz-Pérez, J. C. 2023 Carbon dioxide and light curves and leaf gas
446 exchange responses to shade levels in bell pepper (*Capsicum annuum* L.). *Plant Sci*. **326**, 111532.
447 https://doi.org/10.1016/j.plantsci.2022.111532.
448
449 Keramatlou, I., Sharifani, M., Sabouri, H., Alizadeh, M., Kamkar, B. 2015 A simple linear model for
450 leaf area estimation in Persian walnut (*Juglans regia* L.). *Sci. Hortic*. **184**, 36-39.
451 https://doi.org/10.1016/j.scienta.2014.12.017.
452
453 Klar, A. E. 1984 *Evapotranspiração*. In: A água no sistema solo-planta-atmosfera. São Paulo: Nobel,
454 408 pp.
455
456 Larcher, W. 2003 *Physiological plant ecology*: ecophysiology and stress physiology of functional
457 groups. Berlin, Springer Science & Business Media, 512pp.
458
459 Landsberg, J., Waring, R. 2014 *Forests in our changing world: new principles for conservation and*
460 *management*. Washington, DC, USA: Island Press, 368pp.
461
462 Li, F., Cohen, S., Naor, A., Shaozong, K., Erez, A. 2002 Studies of canopy structure and water use of
463 apple trees on three rootstocks. *Agric. Water Manag*. **55**, 1- 14. https://doi.org/10.1016/S0378-
464 3774(01)00184-6.
465
466 Li, Q., Wei, M., Li, Y., Feng, G., Wang, Y., Li, S., Zhang, D. 2019 Effects of soil moisture on water
467 transport, photosynthetic carbon gain and water use efficiency in tomato are influenced by evaporative
468 demand. *Agric. Water Manag*. **226**, 105818. https://doi.org/10.1016/j.agwat.2019.105818.
469
470 Li, Y., Ming, B., Fan, P., Liu, Y., Wang, K., Hou, P., Xie, R. 2022 Quantifying contributions of leaf
471 area and longevity to leaf area duration under increased planting density and nitrogen input regimens

during maize yield improvement. *Field Crops Res.* **283**, 108551. https://doi.org/10.1016/j.fcr.2022.108551.

Lv, H., Dermann, A., Dermann, F., Petridis, Z., Köhler, M., Saha, S. 2024 Comparable diameter resulted in larger leaf area and denser foliage in the park trees than in street trees: A study on Norway maples of Karlsruhe city, Germany. *Heliyon*, **10**, e23647. https://doi.org/10.1016/j.heliyon.2023.e23647.

Martin-Stpaul, N., Delzon, S., Cochard, H. 2017 Plant resistance to drought depends on timely stomatal closure. *Ecol. Lett.* **20**, 1437-1447. https://doi.org/10.1111/ele.12851.

Martins, F. B., Silva, J. C., Streck, N. A. 2007 Estimativa da temperatura-base para emissão de folhas e do filocrono em duas espécies de eucalipto na fase de muda. *Rev. Árvore*, **31**, 373-381. https://doi.org/10.1590/S0100-67622007000300002.

Martins, F. B., Benassi, R. B., Torres, R. R., De Brito Neto, F. A. 2022 Impacts of 1.5° C and 2° C global warming on *Eucalyptus* plantations in South America. *Sci. Total Environ*, **825**, 153820, 2022. https://doi.org/10.1016/j.scitotenv.2022.153820.

Mattos, E. M., Binkley, D., Campoe, O. C., Alvares, C. A., Stape, J. L. 2020 Variation in canopy structure, leaf area, light interception and light use efficiency among *Eucalyptus* clones. *For. Ecol. Manag*. **463**, 118038. https://doi.org/10.1016/j.foreco.2020.118038.

Meinzer, F. C., Smith, D. D., Woodruff, D. R., Marias, D. E., Mcculloh, K. A., Howard, A. R., Magedman, A. L. 2017 Stomatal kinetics and photosynthetic gas exchange along a continuum of isohydric to anisohydric regulation of plant water status. *Plant, cell, environ*. **40**, 1618-1628. https://doi.org/10.1111/pce.12970.

Muñoz-Villers, L. E., Holwerda, F., Alvarado-Barrientos, M. S., Geissert, D. R., Dawson, T. E. 2018 Reduced dry season transpiration is coupled with shallow soil water use in tropical montane forest trees. *Oecologia*, **188**, 303-317. https://doi.org/10.1007/s00442-018-4209-0.

Nan, G., Wang, N., Jiao, L., Zhu, Y., Sun, H. 2019 A new exploration for accurately quantifying the effect of afforestation on soil moisture: A case study of artificial *Robinia pseudoacacia* in the Loess Plateau (China). *For. Ecol. Manag*. **433**, 459-466, 2019. https://doi.org/10.1016/j.foreco.2018.10.029.

Otto, F. E. L., Coelho, C. A. S., King, A., Perez, E. C., Wada, Y., Oldenborgh, G. J., Haarsma, R., Haustein, K., Uhe, P., Aalst, M. V., Aravequia, J. A., Almeida, W., Cullen, H. 2015 Factors other than climate change, main drivers of 2014/15 water shortage in southeast Brazil. In: Explaining Extremes of 2014 from a Climate Perspective. *Explaining Extreme Events of 2014*, **96**, 3. https://doi.org/10.1175/BAMS-D-15-00120.1.

Pereira, A. R., Angelocci, L. R., Sentelhas, P. C. 2002 *Agrometeorologia*: Fundamentos e aplicações práticas. Porto Alegre: Agropecuária, 294pp.

Pfautsch, S., Bleby, T. M., Rennenberg, H., Adams, M. A. 2010 Sap flow measurements reveal influence of temperature and stand structure on water use of *Eucalyptus regnans* forests. *For. Ecol. Manag*. **259**, 1190-1199. https://doi.org/10.1016/j.foreco.2010.01.006.

Qie, Y. D., Zhang, Q. W., Mcadam, S. A., Cao, K. F. 2024 Stomatal dynamics are regulated by leaf hydraulic traits and guard cell anatomy in nine true mangrove species. *Plant Divers.* **46**, 395-405. https://doi.org/10.1016/j.pld.2024.02.003.

R Development Core Team. R: a language and environment for statistical computing. Vienna, Austria: R Foundation for Statistical Computing, 2022. Disponível em: http://www.R-project.org/. Acesso em: 18 jun 2022.

Rodriguez-Dominguez, C. M., Brodribb, T. J. 2020 Declining root water transport drives stomatal closure in olive under moderate water stress. *New Phytologist*, **225**, 126–134. https://doi.org/10.1111/nph.16177.

Salazar, J. C. S., Melgarejo, L. M., Bautista, E. H. D., Di Rienzo, J. A., Casanoves, F. 2018 Non-destructive estimation of the leaf weight and leaf area in cacao (*Theobroma cacao* L.). *Sci. Hortic*. **229**, 19-24. https://doi.org/10.1016/j.scienta.2017.10.034.

Rossatto, D. R., Silva, L. D. C. R., Villalobos-Vega, R., Sternberg, L. D. S. L., Franco, A. C. 2012 Depth of water uptake in woody plants relates to groundwater level and vegetation structure along a topographic gradient in a neotropical savanna. *Environ. Exp. Bot*. **77**, 259-266. https://doi.org/10.1016/j.envexpbot.2011.11.025.

Scolforo, H. F., Mctague, J. P., Burkhart, H., Roise, J., Campoe, O., Stape, J. L. 2019 Yield pattern of eucalypt clones across tropical Brazil: An approach to clonal grouping. *For. Ecol. Manag*. **432**, 30-39. https://doi.org/10.1016/j.foreco.2018.08.051.

Silva, P. H. M., Junqueira, L. R., De Araujo, M. J., Wilcken, C. F., Moraes, M. L. T., De Paula, R. C. 2020 Susceptibility of eucalypt taxa to a natural infestation by *Leptocybe invasa*. *New Forests*, **51**, 753-763. https://doi.org/10.1007/s11056-019-09758-1.

Sussmilch, F. C., Schultz, J., Hedrich, R., Roelfsema, M. R. G. 2019 Acquiring control: the evolution of stomatal signalling pathways. *Trends Plant Sci*. 24, 342-351. https://doi.org/10.1016/j.tplants.2019.01.002.

553 Stape, J. L., Binkley, D., Ryan, M. G. 2004 *Eucalyptus* production and the supply, use and efficiency of
554 use of water, light and nitrogen across a geographic gradient in Brazil. *For. Ecol. Manag*. **193**, 17-31.
555 https://doi.org/10.1016/j.foreco.2004.01.020.
556
557 Tyree, M. T. 1988 A dynamic model for water flow in a single tree: evidence that models must account
558 for hydraulic architecture. *Tree Physiol*. **4**, 195-217, 1988. https://doi.org/10.1093/treephys/4.3.195.
559
560 Urban, J., Ingwers, M. W., Mcguire, M. A., Teskey, R. O. 2017 Increase in leaf temperature opens
561 stomata and decouples net photosynthesis from stomatal conductance in Pinus taeda and *Populus*
562 *deltoides* x *nigra*. *J. Exp. Bot*. **68**, 1757-1767, 2017. https://doi.org/10.1093/jxb/erx052.
563
564 Vadez, V., Kholová, J., Hummel, G., Zhokhavets, U., Gupta, S. K., Hash, C. T. 2015 LeasyScan: a novel
565 concept combining 3D imaging and lysimetry for high-throughput phenotyping of traits controlling
566 plant water budget. *J. Exp. Bot*. **66**, 5581-5593. https://doi.org/10.1093/jxb/erv251.
567
568 Wang, L., Good, S. P., Caylor, K. K. 2014 Global synthesis of vegetation control on evapotranspiration
569 partitioning. *Geophys. Res. Lett*. **41**, 6753-6757. https://doi.org/10.1002/2014GL061439.
570
571 Wang, X., Ye, T., Ata-Ul-Karim, S. T., Zhu, Y., Liu, L., Cao, W., Tang, L. 2017 Development of a
572 critical nitrogen dilution curve based on leaf area duration in wheat. *Front. Plant Sci*. **8**, 1517.
573 https://doi.org/10.3389/fpls.2017.01517.
574
575 Wei, Z., Yoshimura, K., Wang, L., Miralles, D. G., Jasechko, S., Lee, X. 2017 Revisiting the
576 contribution of transpiration to global terrestrial evapotranspiration. *Geophys. Res. Lett*. **44**, 2792-2801.
577 https://doi.org/10.1002/2016GL072235.
578

White, D. A., Dunin, F. X., Turner, N. C., Ward, B. H., Galbraith, J. H. Water use by contour-planted belts of trees comprised of four *Eucalyptus* species. *Agric. Water Manag*. **53**, 133-152, 2002. https://doi.org/10.1016/S0378-3774(01)00161-5.

Wullschleger, S. D., Meinzer, F. C., Vertessy, R. A. 1998 A review of whole-plant water use studies in tree. *Tree physiol*. 18, 499-512. https://doi.org/10.1093/treephys/18.8-9.499.

Yi, Y., Yano, K. 2023 Nocturnal versus diurnal transpiration in rice plants: Analysis of five genotypes grown under different atmospheric CO_2 and soil moisture conditions. *Agric. Water Manag*. **286**, 108397. https://doi.org/10.1016/j.agwat.2023.108397.

Zhang, H., Wei, W., Chen, L., Wang, L. Effects of terracing on soil water and canopy transpiration of *Pinus tabulaeformis* in the Loess Plateau of China. *Ecol. Eng*. v. 102, p. 557-564, 2017. https://doi.org/10.1016/j.ecoleng.2017.02.044.

Zhang, D., Du, Q., Zhang, Z., Jiao, X., Song, X., LI, J. 2017 Vapour pressure deficit control in relation to water transport and water productivity in greenhouse tomato production during summer. *Sci. Rep*. **7**, 43461.

Zhang, Z.; Zhao, P.; Zhao, X.; Zhou, J.; Zhao, P.; Zeng, X.; Ouyang, L. 2018 The tree height-related spatial variances of tree sap flux density and its scale-up to stand transpiration in a subtropical evergreen broadleaf forest. *Ecohydrology*, **11**, e1979. https://doi.org/10.1002/eco.1979.

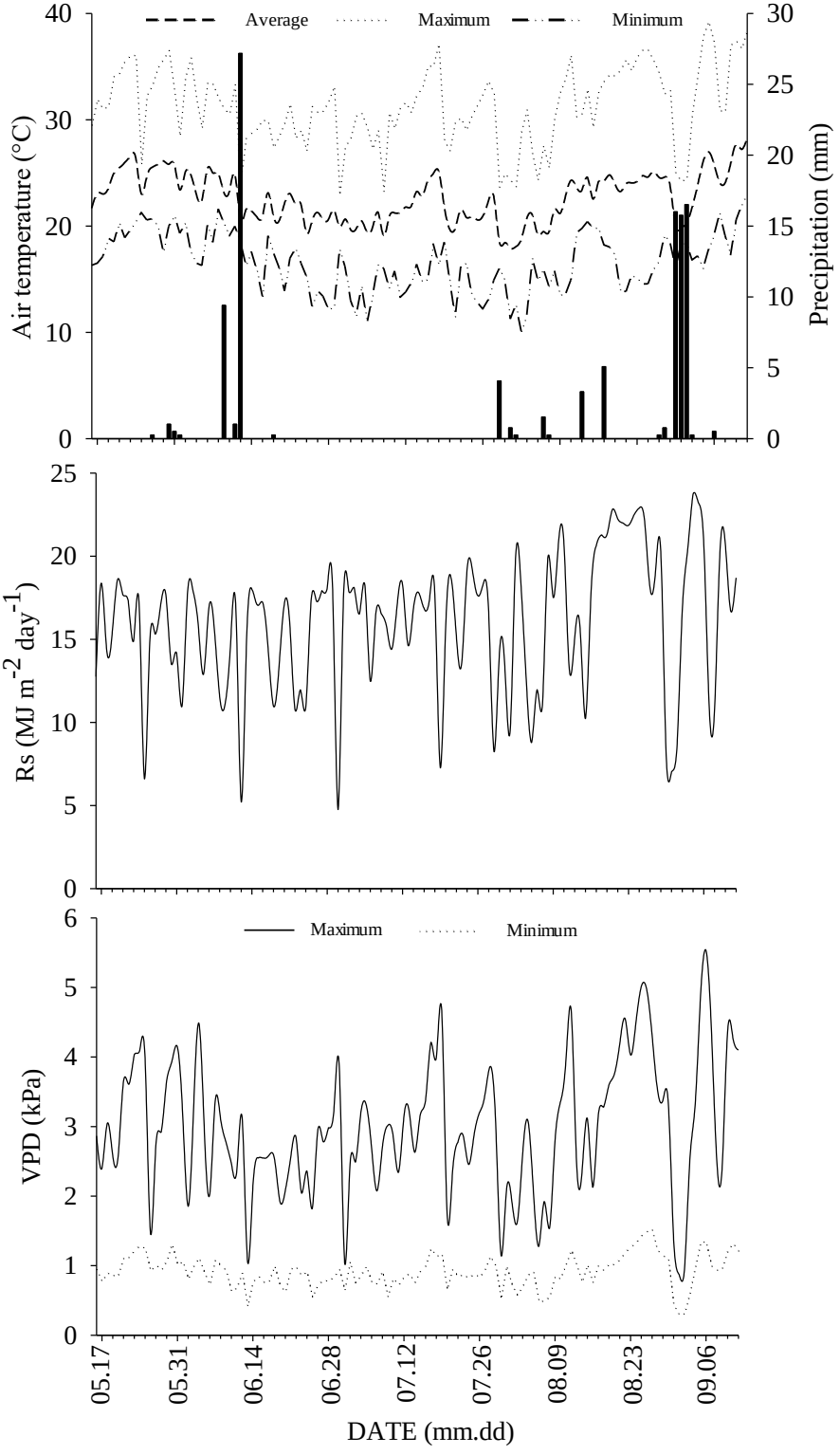

Figure 1. Daily air temperature, precipitation, global radiation (Rs) and vapor pressure deficit (VPD) during the experimental period, between May 16th and September 12th, 2021, in Jerônimo Monteiro city, Espírito Santo state, Brazil.

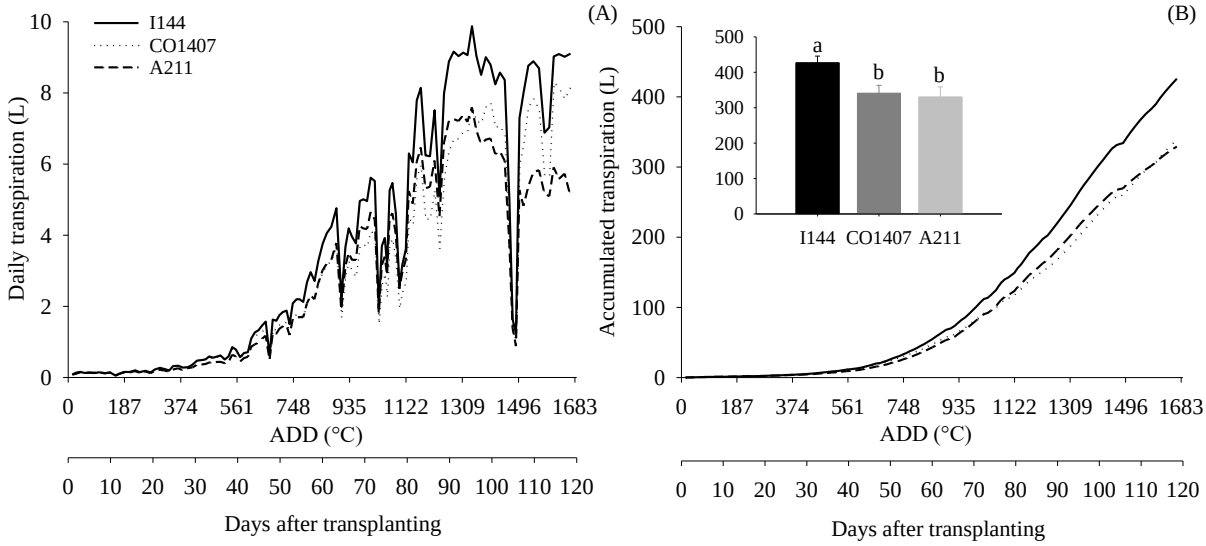

Figure 2. Time course of daily transpiration (A) and accumulated transpiration (B) of young plants of three *Eucalyptus* clones based on accumulated degree days (ADD) and days after transplanting. Lowercase letters compare means of accumulated transpiration of *Eucalyptus* clones at the end of the experiment, calculated by ADD, using Tukey's test ($p < 0.05$).

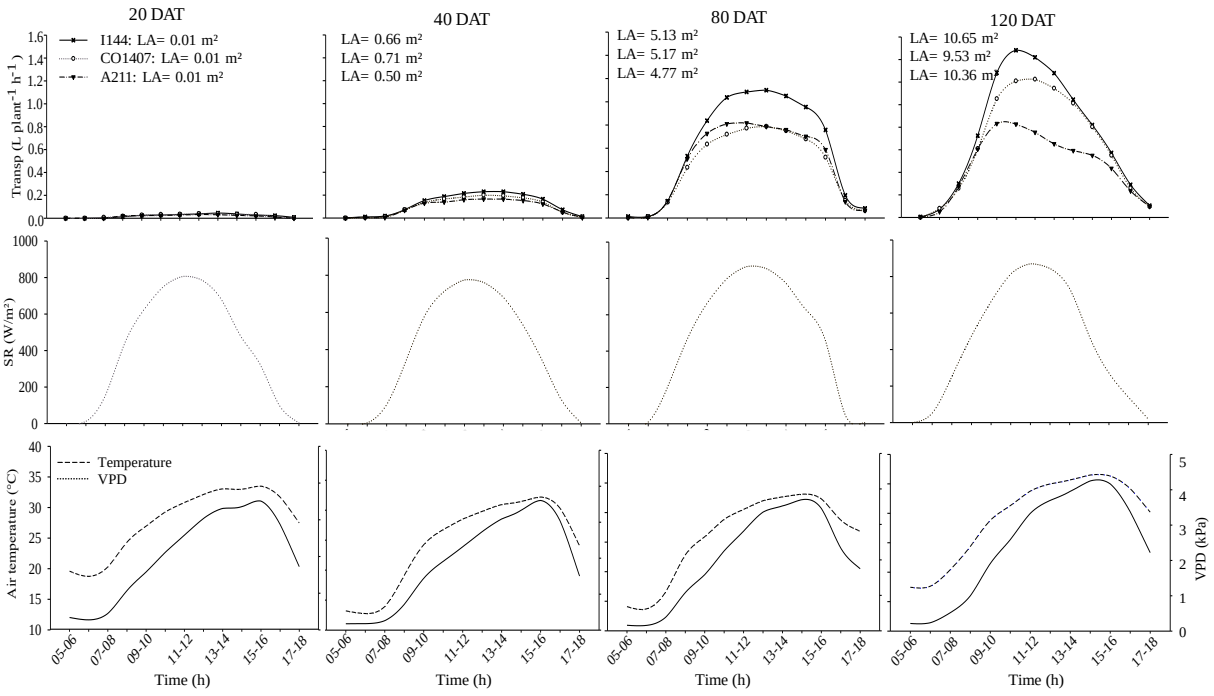

Figure 3. Hourly measurements on transpiration of young plants of *Eucalyptus* clones, global solar radiation (SR), air temperature, and vapor pressure deficit (VPD) at 20, 40, 80 and 120 DAT. Leaf area (LA) data of clones are attached to transpiration measurements.

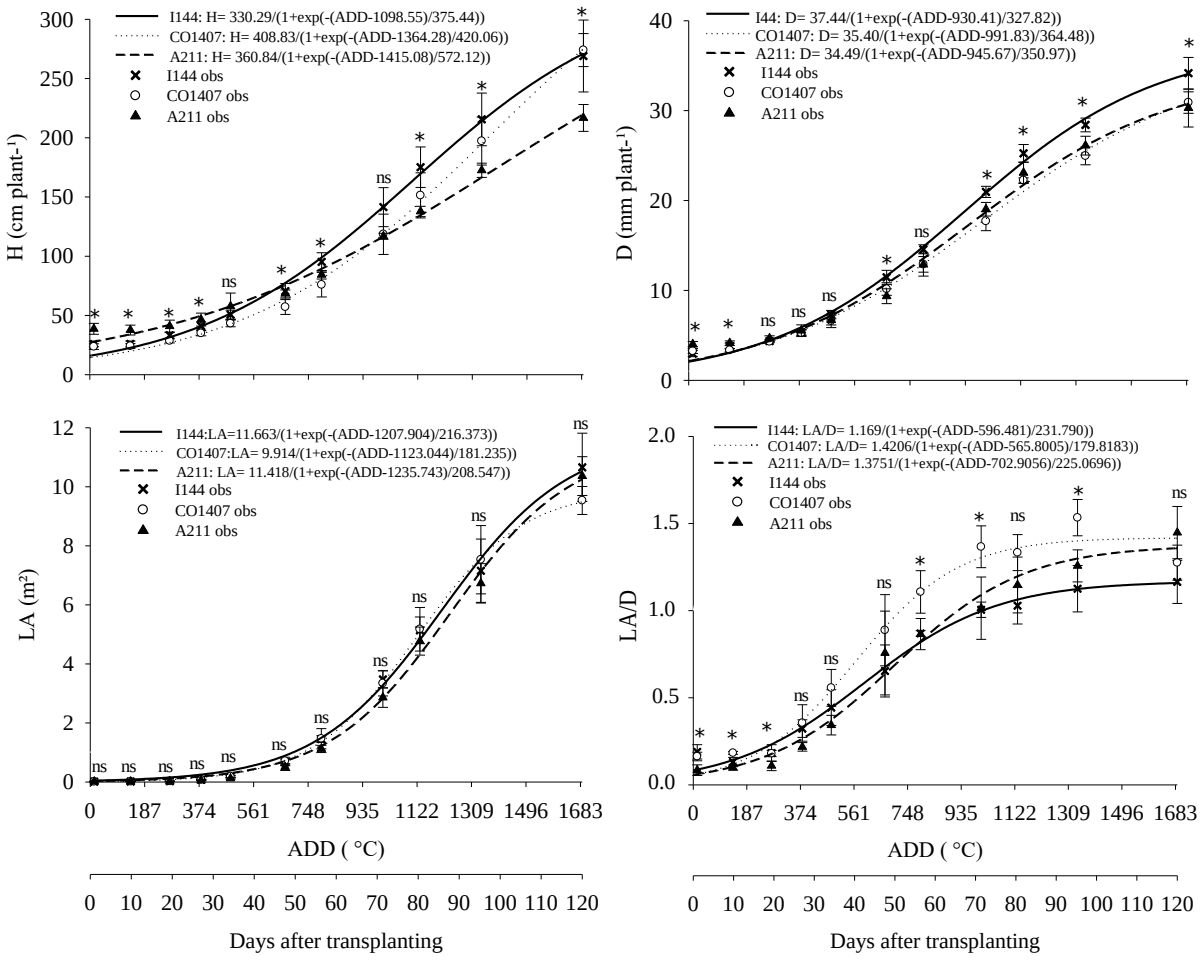

Figure 4. Plant height (H), stem diameter (D), leaf area (LA), and leaf area/stem diameter ratio (LA/D) in young plants of *Eucalpytus* clones, based on accumulated degree days (ADD) and days after transplanting ($0.97 \leq R^2 \leq 0.99$). (*) significant and (^{ns}) not significant, by F test ($p < 0.05$). The bars indicate the standard error of means.

Table 1. Dry mass of leaves (LDM), branches (BDM), roots (RDM), and total (TDM) and water use efficiency (WUE) of *Eucalyptus* clones at the end of the experimental period.

Clones	LDM (g)	BDM (g)	RDM (g)	TDM (g)	WUE (kg m^{-3})
I144	567.59 a	756.56 a	194.02 a	1518.18 a	3.90 b
CO1407	488.98 a	581.59 b	141.63 b	1212.21 b	3.95 ab
A211	504.22 a	641.41 ab	176.46 ab	1322.09 ab	4.31 a

* Lowercase letters compare clones within each trait, using Tukey's test ($p \leq 0.05$).

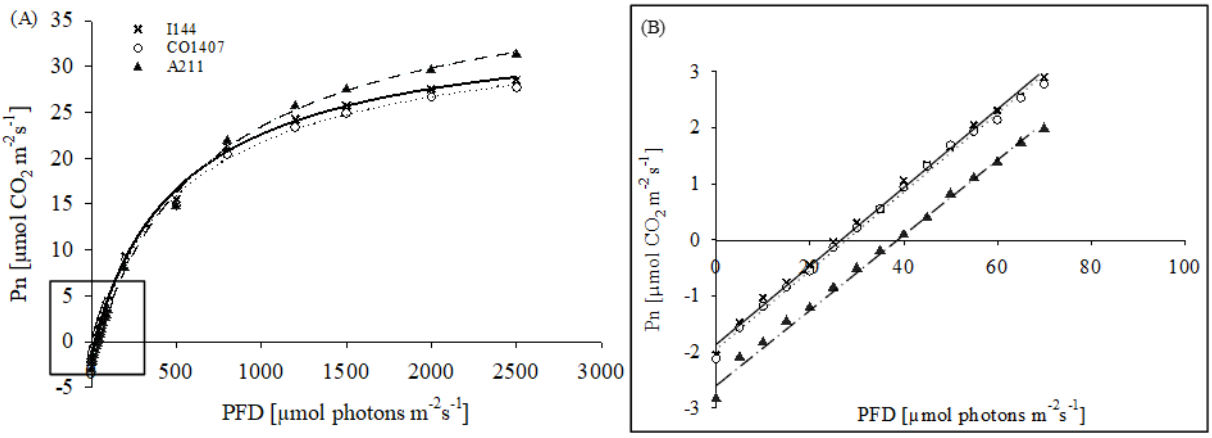

Figure 5. Photosynthesis response curve (A) and light compensation point zoom represented by the square (B) in young plants of *Eucalyptus* clones. The solid and dashed black lines represent data fit using the hyperbolic model. Pn = net photosynthesis rate; PFD = photosynthetic photon flux density.

Table 2. Photosynthetic parameters derived from response curves to photosynthetically active radiation in young plants of *Eucalyptus* clones: maximum net photosynthesis (A_{max}); dark respiration (R_d); apparent quantum yield (Φ); light compensation point (LCP), and light saturation point (LSP).

Photosynthetic parameters	Clones		
	I144	CO1407	A211
A_{max} [µmol (CO_2) m^{-2} s^{-1}]	37.43 b	37.37 b	43.51 a
R_d [µmol (CO_2) m^{-2} s^{-1}]	1.95 a	2.07 a	2.52 a
Φ [mol (CO_2) mol^{-1} (photons)]	0.08 a	0.08 a	0.07 b
LCP [µmol (photons) m^{-2} s^{-1}]	25.93 a	26.54 a	38.14 a
LSP [µmol (photons) m^{-2} s^{-1}]	1922.20 a	1922.75 a	1918.92 a

* Lowercase letters compare clones within each photosynthetic parameter, using Tukey's test ($p \leq 0.05$).

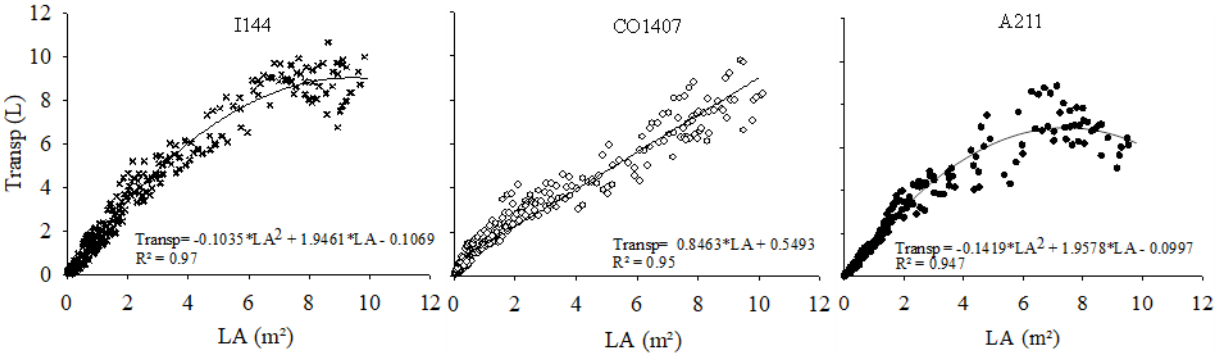

652

653 **Figure 6.** Relationship between transpiration (Transp.) and leaf area (LA) in young plants of *Eucalyptus*
654 clones on days with no precipitation and low cloudiness during the experimental period.
655

656

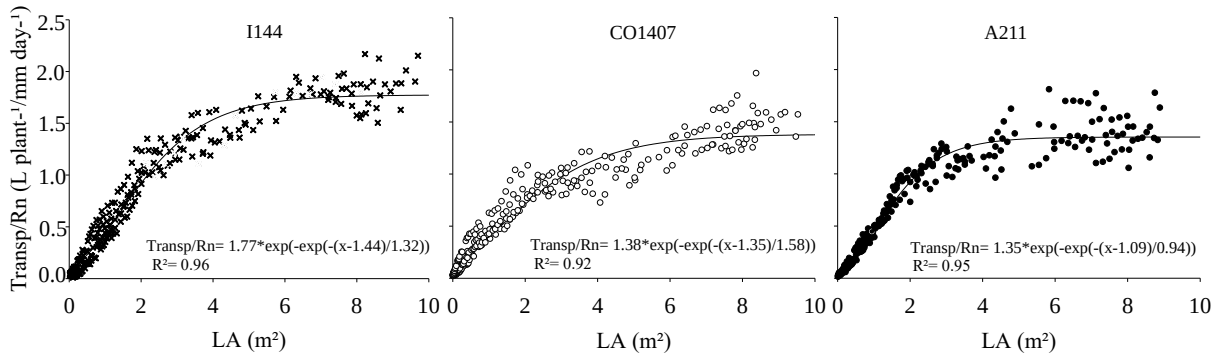

657

658 **Figure 7.** Daily transpiration (Transp) / available radiation (Rn) ratio based on leaf area (LA) of young
659 plants of *Eucalyptus* clones on days with no precipitation and low cloudiness during the experimental
660 period.
661

662